Influence of Buoyancy Module Characteristics on Free Vibration Response of Steep Wave Riser (SWR)

Supamit Supabut[1,*] Karun Klaycham[2]

[1,2] Department of Civil Engineering, Faculty of Engineering at Kamphaengsaen, Kasetsart University Kamphaengsaen Campus, Nakhon Pathom, THAILAND

**Corresponding author; E-mail address: supamit.su@ku.ac.th*

Abstract

In the petroleum industry, subsea pipelines transporting crude oil from wellheads to production platforms are subjected to harsh environmental conditions and external forces that affect their structural integrity. High-stress concentrations often occur at the points where the pipeline touches the seabed, potentially leading to structural failure. To mitigate this issue, small buoyancy modules are strategically attached along sections of the pipeline to provide additional buoyant force, preventing direct contact with the seabed. The configuration of this riser system is called the "Steep Wave Riser (SWR)". This paper aims to present a three-dimensional static and dynamic analysis of SWR pipelines using an elastic rod model, developed based on force and moment equilibrium principles. The model incorporates the effects of external forces, including hydrodynamic forces from water currents, hydrostatic pressure, buoyancy forces from the pipeline and floaters, self-weight, and internal fluid forces. The equilibrium equations are formulated in a Cartesian coordinate system and expressed as nonlinear differential equations, which are solved numerically using the Galerkin finite element method in conjunction with the Newton-Raphson iterative approach. Additionally, the free vibration characteristics of the SWR are analyzed using the eigenvalue problem-solving method to investigate the system's dynamic behavior. Finally, the analysis focuses on optimizing the buoyancy module parameters to enhance the structural stability of SWR pipelines, minimize failure risks, and ensure efficient performance under complex subsea environmental conditions.

Keywords: Cartesian coordinate system / Eigenvalue problem / Elastic rod / Steep Wave Risers / Newton-Raphson iterative method

1. Introduction

Currently, the offshore petroleum drilling industry has expanded into deep-water regions to explore crude oil and natural gas. Therefore, the length of the riser made from steel, particularly the traditional steel catenary riser (SCR), has increased. The SCR has very high tensile forces at the top of the riser. Additionally, the movement at the end of the pipe on the water surface and the harsh environmental conditions lead to high structural stress and significant fatigue at the Hang-off point and the touchdown zone (TDZ). This makes the SCR reasonably unsuitable for the transportation or production of crude oil and natural gas [1-3].

A model for the interaction between the riser and the seabed has been developed to describe the characteristics and interactions between the SCR and the seabed. Most of these models typically employ stress analysis methods [4-5]. A model related to the behavior between the soil and the riser was presented by Zhou et al. [6]. This model is based on the effective-stress principle [7-8] and utilizes theory of soil mechanics in a critical state. This helps to simplify the calculation process by establishing a relationship between soil strength and changes in effective stress as forces are repeatedly applied between the SCR and the soil. This model can be used to describe the interaction between the SCR and the soil more comprehensively, including the behavior of the subsea. The latest model that analyzes the dynamic response and fatigue damage of the SCR at the touchdown zone (TDZ) has been presented by Gao et al [9]. This model simulates the behavior between the soil and the riser, using the effective stress principle to evaluate the changes in soil strength due to the movement of the embedded section of the SCR. Kim et al [10] presented the instability caused by both internal and external motion of the pipe, and investigated the natural frequency of catenary-type risers to assess the risk of resonance between the riser and sea waves, which could lead to harmful vibrations affecting the riser's structure.

Bai [11] developed the riser system called the Wave Riser, which is constructed by installing buoyancy modules on a Steel Catenary Riser (SCR) to form a curved section. The wave risers (WRs) help in reduction of the tensile force and moment at the end or the hang-off point where the riser contacts the seabed (Touchdown Zone, TDZ). These systems are referred to as the steep wave risers (SWR) and the lazy wave risers (LWR). Qiao et al [12] conducted a study on the nonlinear static analysis of the SWR in an environment influenced by current forces, studying

the impact of current-induced forces on the behavior and response of the riser in a two-dimensional (2D) configuration.

From the review of all the research, it was found that the analysis of the free vibration of steep wave risers has not been studied in detail when the length of the riser is large, and the physical characteristics of the buoyancy modules influence the shape, weight, and internal forces of the riser. As shape and characteristics of the steep wave riser shown in **Fig. 1**, it is divided into three sections along the arc length of the riser including the decline section (L_1), the buoyancy section (L_2) and the hang-off section (L_3). Then the total arc length of the riser (L) is given by $L = L_1 + L_2 + L_3$.

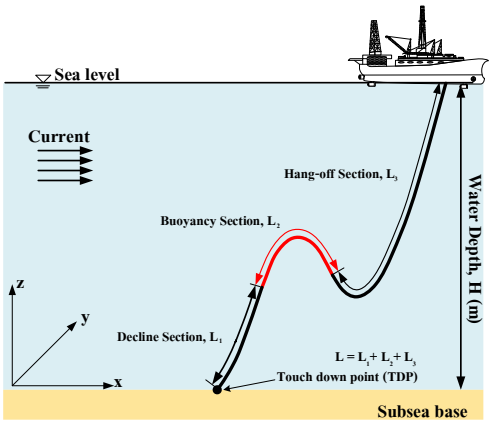

Fig. 1 Steep wave riser (SWR) system

The main objective of this research is to develop a mathematical model for the steep wave riser using the principles of force and moment equilibrium and to analyze numerical solutions using the finite element method. Since the system of equations is nonlinear, the Newton-Raphson iterative process is used to find the numerical solutions. The natural frequency of the SWR is determined using the eigenvalue problem solver. Then the accuracy of the numerical results are verified by comparing them with other related research studies.

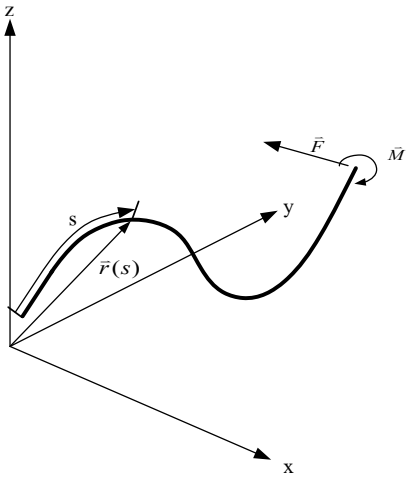

Fig. 2 Coordinate System of Steep wave riser (SWR)

2. Elastic Rod Theory

2.1 Coordinate System

When considering a steep wave riser as a space curve and letting $\vec{r}$ be the position vector at any point of centroidal line of riser, which is a function of the arc length along the central axis of the SWR in three dimensions, $\hat{t}$ is the unit tangent vector to the curve, $\hat{n}$ is the unit normal vector to the curve, and $\hat{b}$ is the unit binormal vector to the curve. as shown in **Fig. 2**

2.2 Elastic Rod Balance Equation

Fig. 3 shows a differential segment of the SWR in equilibrium state, where $\vec{F}$ is the vector of the resultant internal force of the differential segment, $\vec{M}$ is the vector of the resultant internal moment of the differential segment, $\vec{q}$ is the vector of the external force per unit length, s is the arc length coordinate and $\vec{m}$ is the vector of the external moment per unit length.

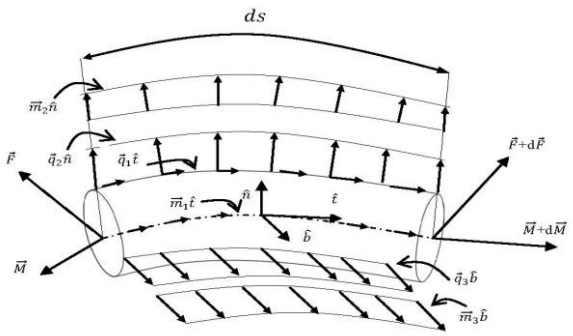

Fig. 3 Free body diagram of differential segment of steep wave riser

According to Newton's second law, the sum of the vectors of the resultant force and moment can be expressed in the form of Eqs. (1) and (2), respectively.

$$\vec{F}' + \vec{q} = (m_a + m_f)\ddot{\vec{r}} \tag{1}$$

$$\vec{M}' + \vec{r}' \times \vec{F} + \vec{m} = 0 \tag{2}$$

The superscripts $'$ and $'$ above the parameter denote the derivative with respect to the arc length coordinate (s) and the time (t), respectively. The symbols $\vec{r}$ and $\ddot{r}$ are the vector of riser position and riser acceleration, respectively, m_a and m_f are the mass of the riser and the mass of the internal fluid within the riser, respectively. The rod is assumed to be elastic and extensible, therefore the deformation condition holds:

$$\frac{1}{2}[\vec{r}' \cdot \vec{r}' - 1] = \frac{[\tilde{\lambda} - (\rho_o A_o - \rho_i A_i) + \rho_i A_i v_i^2]}{EA} = \varepsilon_t \tag{3}$$

where $\lambda = T_e - EI\kappa^2$, $\kappa = r''$ is the local curvature, $T_e = T + \rho_o A_o - \rho_i A_i$ is the local effective tension, T is the wall tension, ρ_o and ρ_i are the external and internal hydrostatic pressures, respectively, A_o and A_i are the outer and inner cross-sectional areas, respectively, EA is the axial tensile stiffness of SWR, A is the cross-sectional area, v_i is the relative velocity of internal fluid in tangential direction.

From the equilibrium equation of an elastic rod Eqs. (1) and (2), the equation of motion of the SWR can be written as:

$$-(EI\vec{r}'')'' + (\lambda\vec{r}')' + \vec{q} = (m_a + m_f)\ddot{\vec{r}} \tag{4}$$

2.3 Load Analysis in SWR

The external forces acting on the SWR consist of the riser weight, the hydrostatic pressure, the hydrodynamic forces of current and wave, and the force caused by internal fluid motion. These forces can be expressed by the following equations.

$$\vec{q} = \vec{w} + \vec{F}^s + \vec{F}^d \tag{5}$$

where $\vec{q}$ is the vector of the external force per unit length, $\vec{w}$ is the effective weight of the riser per unit length, $\vec{F}^s$ is the hydrostatic pressure per unit length and $\vec{F}^d$ is the hydrodynamic force per unit length.

2.2.1 Buoyancy Force

Buoyancy modules are installed along a specific section of the riser, referred to as the buoyancy segment with length of L_2. Most buoyancy materials used have a lower density than water, such as foam or thin-walled buoyancy modules filled with air. These materials help provide uniform buoyant force to the riser, preventing any part of the riser from coming into contact with the seabed. The shape of the buoy is shown in **Fig. 4**

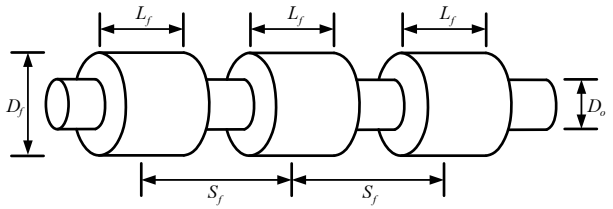

Fig. 4 Shape and physical characteristics of the buoy

The effective weight of the buoyancy segment can be expressed as follows.

$$\vec{w} = \vec{w}_p + \vec{w}_b \tag{6}$$

where $\vec{w}_p$ and $\vec{w}_b$ are the submered weight of the riser and the buoyant force of buoyancy module, respectively.

$$\vec{w}_p = (\rho_w A_o - \rho_i A_i - \rho_p A_p)g \tag{7}$$

$$\vec{w}_b = \frac{\frac{\pi}{4}\left[(\rho_w L_f\left(D_f^2 - D_o^2\right)) - (\rho_b L_f\left(D_f^2 - D_o^2\right) + m_{fh})\right]g}{S_f} \tag{8}$$

where ρ_w, ρ_i and ρ_p are the densities of the seawater, the internal transporting fluid, and the riser, respectively, A_p is the cross-sectional area of the riser, D_f and D_o are the buoyancy block diameter and external diameter of the riser, respectively, L_f is the length of buoyancy block, S_f is a pitch of buoyancy block and m_{fh} is the attached rigging mass of buoyancy block.

3. Finite Element Model

From Eqs. (3), (4) and (5), the equation of motion of the SWR can be written in subscript notation as follows:

$$-\left(m_a + m_f\right)\ddot{r}_i - C_A\ddot{r}_i - 2m_f v_{in}\dot{r}_i' - \left(EI\vec{r}_i''\right)'' + (\lambda\vec{r}_i')' + \bar{w}_i + \bar{F}_i^d = 0 \tag{9}$$

$$\frac{1}{2}[\vec{r}' \cdot \vec{r}' - 1] - \frac{\lambda - P + m_f {v_{in}}^2}{EA} = 0 \tag{10}$$

where $i =$ 1,2,3. The SWR is discretized into a number of elements along the arc length. The riser position and axial tension at any point in the riser element can approximated by the following subsequent equations.

$$r_i(s) = N_l U_{il} \tag{11}$$

$$\lambda(s) = P_m \lambda_m \tag{12}$$

where $i =$ 1,2,3 $l =$ 1,2,3,4 and $m =$ 1,2, respectively. N_l are the Hermitian cubic shape functions, P_m are the Hermitian quadratic shape functions, U_{il} are the position and tangent vectors, and λ_m are the effective tension vectors. The final equations for the SWR vibration are as follows:

$$\left(M_{ijlk} + M_{ijlk}^a\right)\ddot{U}_{jk} + \left(C_{ijlk}^f + G_{ijlk}\right)\dot{U}_{jk} + \left(K_{ijlk}^1 + \lambda_n K_{nijlk}^2\right)U_{jk} - F_{il} = 0 \tag{13}$$

$$A_{mil}U_{ki}U_{kl} - B_m + C_{mn}(h_n - \lambda_n) = 0 \tag{14}$$

where M_{ijlk} and M_{ijlk}^a are the mass matrices, K_{ijlk}^1 and K_{nijlk}^2 are the stiffness matrices, resisting axial stretching and bending deformation, respectively, C_{ijlk}^f is a damping matrix induced by hydrodynamic force, G_{ijlk} is a gyroscopic matrix by internal flow, F_{il} is an external load vector, $A_{mil} = \frac{1}{2}\int_0^L P_m A_i' A_l' ds$, $B_m = \frac{1}{2}\int_0^L P_m ds$, $C_{mn}\frac{1}{EA}\frac{1}{2}\int_0^L P_m P_n ds$ and $h_n = \rho_o A_o - \rho_i A_i$. where $i, j =$ 1,2,3 are the three directions of node motion (i.e., x, y, z). $l, k =$ 1, 2, 3, 4 are the numbers of the Hermitian cubic shape functions and $m, n =$ 1, 2 corresponding to the Hermitian quadratic shape functions.

4. Nonlinear Static Analysis

For the static analysis of the SWR, the time dependent forces are neglected from the governing equation, one obtains:

$$R_{ij} = \left(K^1_{ijlk} + \lambda_n K^2_{nijlk}\right)U_{jk} - F_{il} = 0 \quad (15)$$

$$G_m = A_{mil}U_{ki}U_{kl} - B_m + C_{mn}(h_n - \lambda_n) = 0 \quad (16)$$

Since Eqs. (15) and (16) form a nonlinear system of equations, the Newton-Raphson method will be used to solve the problem numerically. The Taylor series is employed for approximation, and the derivatives of order higher than the second order are neglected. The system of equations can then be written in the matrix form as follows:

$$R^{(n+1)}_{il} = R^{(n)}_{il} + \frac{\partial R_{ij}}{\partial U_{jk}}\left(\Delta U_{jk}\right) + \frac{\partial R_{ij}}{\partial \lambda_n}(\Delta\lambda_n) = 0 \quad (17)$$

$$G^{(n+1)}_{m} = G^{(n)}_{m} + \frac{\partial G_m}{\partial U_{jk}}\left(\Delta U_{jk}\right) + \frac{\partial G_m}{\partial \lambda_n}(\Delta\lambda_n) = 0 \quad (18)$$

From the iterative process, the system of Eqs. (17) and (18) will be solved iteratively until the values of ΔU_{jk} and $\Delta\lambda_n$ converge to zero with acceptable error criterion.

5. Free Vibration Analysis

For free vibration analysis, the hydrodynamic damping force and excitation force are neglected from the equation of motion, then the equation for free vibration is expressed by

$$\left(M_{ijlk} + M^a_{ijlk}\right)\ddot{U}_{jk} + \left(G_{ijlk}\right)\dot{U}_{jk} + \left(K^1_{ijlk} + \lambda_n K^2_{nijlk}\right)U_{jk} = 0 \quad (19)$$

The equation can be formulated in the form of an eigenvalue problem as follows:

$$\left(K^1_{ijlk} + \lambda_n K^2_{nijlk}\right)\{\varphi\} = \omega^2\left(M_{ijlk} + M^a_{ijlk}\right)\{\varphi\} + \omega(G_{ijlk})\{\varphi\} \quad (20)$$

where ω is the natural frequency of the SWR, and $\{\varphi\}$ is the corresponding free vibration mode shape. The solution is obtained using the eigenvalue method to solve the problem in MATLAB.

6. Numerical Validation

The analysis results are compared with research by Qiao et al. [12] and Kim et al. [10] to verify the accuracy of the mathematical model and computational process used in this study. The detailed physical properties of the SWR used in this study are presented in **Table 1.** In this section, two validation examples are presented, including static analysis of the SWR and natural frequency analysis of the SCR.

Table 1 Properties of riser and environmental condition used in numerical validation.

Properties	Unit	Model 1[a]	Model 2[b]
Horizontal offset	m	1018	450
Vertical offset	m	0	0
Sea depth	m	1500	900
Length of decline section	m	450	-
Length buoyancy section	m	672	-
Length hang-off section	m	1076	-
Total arc length	m	2198	1000 - 2600
Density of riser	kg/m^3	7850	7850
Density of external fluid	kg/m^3	1025	1025
Density of internal fluid	kg/m^3	998	998
Density of buoyancy block	kg/m^3	1	-
Buoyancy block diameter	m	0.46	-
Outer diameter of riser	m	0.22	0.26
Inner diameter of riser	m	0.2	0.2
Current velocity in x-direction	m/s	0.2	0
Internal fluid velocity	m/s	0	0
Length of buoyancy block	m	1	-
Attached rigging mass of buoyancy block	kg	0	-
Pitch of the buoyancy block	m	1	-

[a] Qiao et al. [12].
[b] Kim et al. [10].

For the first validation example, the static analysis of the SWR was analyzed and compared with the study by Qiao et al. [12]. The riser properties and environmental conditions in **Table 3** are used (Model 1). The obtained results are similar, with discrepancies primarily observed in the buoyancy section. The shape deviation is quantified at 0.5%, as illustrated in **Fig. 5**, while the deviation in top tension is 0.5%, as shown in **Fig. 6**.

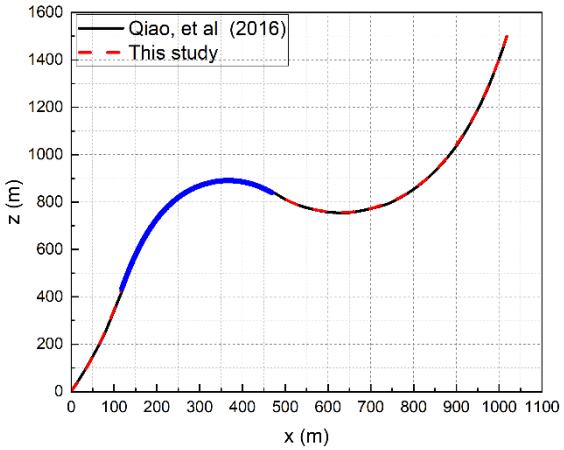

Fig. 5 Comparison of the SWR configuration

For the second validation example, the free vibration analysis of the SCR is simulated using environmental conditions of Model 2 in **Table 3**, and compared the numerical results with Kim et al. [10]. **Fig. 7** presents the effect of top tension on the total length of the riser, in comparing with Kim et al. [10]. It illustrates that the critical top tension (point 5 in **Fig. 7**) of the riser is the

minimum force required to maintain the riser in an equilibrium state. If the top tension is less than this critical top tension, the riser cannot achieve the equilibrium. Conversely, if the top tension exceeds the critical top tension, the riser can attain two types of equilibrium states: stable equilibrium and unstable equilibrium. The equilibrium state with a shorter total arc length is the stable equilibrium, while the one with a longer total arc length is the unstable equilibrium.

Table 2 First two natural frequencies of the SCR riser (Model 2)

No. of Conf.	Top Tension [kN]	Natural frequencies, ω [rad/s]					
		1st Mode			2nd Mode		
		Kim et al. [10]	Present	%Diff	Kim et al. [10]	Present	%Diff
(1)	2500	0.2582	0.2579	0.13%	0.5165	0.5159	0.12%
(2)	2200	0.2332	0.2330	0.08%	0.4665	0.4661	0.08%
(3)	1900	0.2036	0.2039	-0.17%	0.4072	0.4080	-0.19%
(4)	1600	0.1617	0.1630	-0.81%	32.32%	0.3258	-0.81%
(5)*	**1525**	0.1350	0.1349	0.08%	0.2682	0.2682	0.02%
(6)	1600	0.1146	0.1138	0.71%	0.2228	0.2214	0.62%
(7)	1900	0.0949	0.0949	0.00%	0.1728	0.1731	-0.17%
(8)	2200	0.0848	0.0852	-0.51%	0.1456	0.1466	-0.70%
(9)	2500	0.0777	0.0779	-0.25%	0.1274	0.1279	-0.40%

(5)* is the critical top tension.

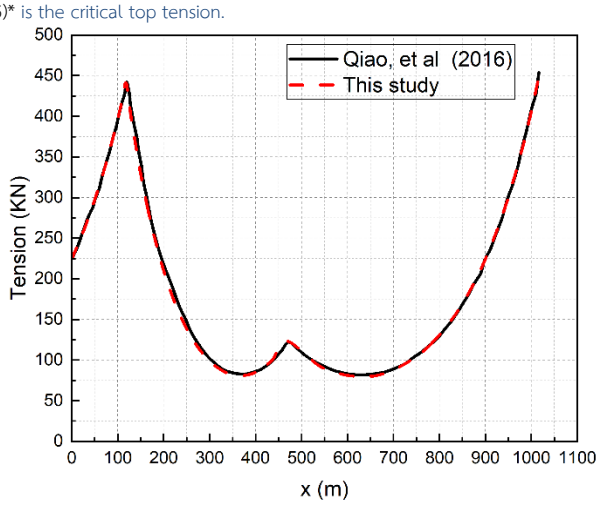

Fig. 6 Comparison of the tension distribution in SWR.

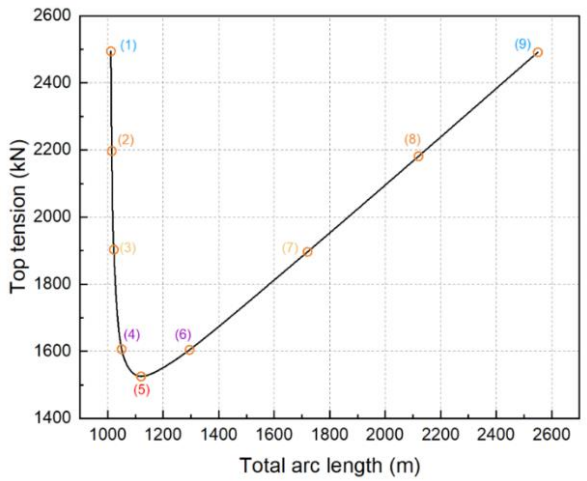

Fig. 7 Relation between tension at the hang-off point and SCR length

The natural frequency for the first two mode of the riser was compared with the study by Kim et al. [10]. The comparison of the numerical results show an acceptable agreement with maximum percent different of 0.81, as presented in **Table 2** and **Fig. 7**.

7. Results and Discussions

The properties of SWR and the environmental conditions used in numerical simulation are presented in **Table 3**.

Table 3 Properties of SWR and environmental condition used in numerical simulation.

Properties	Unit	Case 1	Case 2
Horizontal offset	m	600	600
Vertical offset	m	0	0
Sea depth	m	1200	1200
Length of decline section	m	300	300
Length of buoyancy section	m	700	500-900
Length of hang-off section	m	500	300-700
Total arc length	m	1500	1500
Density of riser	kg/m^3	7850	7850
Density of external fluid	kg/m^3	1025	1025
Density of internal fluid	kg/m^3	998	998
Density of buoyancy block	kg/m^3	1	1
Buoyancy block diameter	m	0.40-0.60	0.50
Outer diameter of SWR	m	0.22	0.22
Inner diameter of SWR	m	0.20	0.2
Current velocity in x-direction	m/s	–	–
Internal fluid velocity	m/s	–	–
Length of buoyancy block	m	1	1
Attached rigging mass of buoyancy block	kg	0	0
Pitch of the buoyancy block	m	1	1

7.1 Effects of Buoyancy Diameter

This subsection investigates the effect of buoyancy diameter on the static equilibrium and free vibration behavior of the steep wave riser with different five diameters: 0.40 m, 0.45 m, 0.50 m, 0.55 m, and 0.60 m. The parameters used for this analysis is given in **Table 3** (case 1).

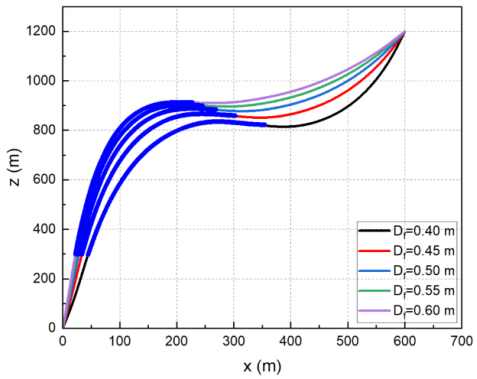

Fig. 8 Effect of Buoyancy diameter on the static equilibrium configuration

The results demonstrate a correlation with the increase in buoyancy diameter and the resultant riser shape. Specifically, the curvature of the wave riser section rises as the buoyancy diameter increases, as shown in **Fig. 8**. The internal tension of the riser in the section without buoys also increases with the increase in buoyancy diameter, as shown in **Fig. 9**.

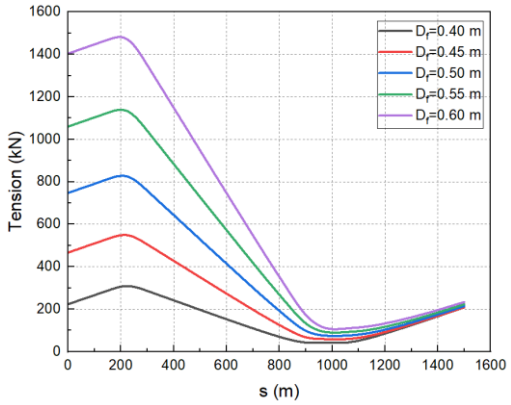

Fig. 9 Effect of buoyancy diameter on the distribution of internal tension

Additionally, the natural frequency of the SWR is presented in **Table 4**. In this study, only the first 10 vibration modes are presented. The corresponding free vibration mode shapes of the steep wave riser (SWR) are shown in **Fig. 10-12**, as an example for case of 0.50 m buoyancy diameter**.** The in-plane vibration mode shape in x- directions and z-directions are shown in **Fig. 10**, respectively, while the out-of-plane mode shape (y-direction) is shown in **Fig. 10**.The analysis indicates that the free vibration of the in-plane SWR results in both in-plane and out-of-plane lateral vibrations. From the vibration sequential mode and the riser's natural frequencies, it is found that out-of-plane vibrations are more likely to occur and precede in-plane vibrations.

Table 4 Effect of buoyancy diameter on the natural frequency of SWR

Diameter (m)	Natural frequencies, ω [rad/s]									
	Out-of-plane mode					In-plane mode				
	1st Mode	3rd Mode	5th Mode	7th Mode	9th Mode	2nd Mode	4th Mode	6th Mode	8th Mode	10th Mode
0.40	0.0772	0.1309	0.1943	0.2562	0.3255	0.0826	0.1511	0.2251	0.2646	0.3608
0.45	0.0944	0.1564	0.2358	0.3109	0.3911	0.1002	0.1882	0.2615	0.3336	0.4387
0.50	0.1088	0.1784	0.2710	0.3570	0.4472	0.1160	0.2212	0.2934	0.3986	0.4913
0.55	0.1218	0.1984	0.3026	0.3986	0.4985	0.1306	0.2525	0.3233	0.4605	0.5358
0.60	0.1339	0.2176	0.3321	0.4379	0.5468	0.1446	0.2825	0.3528	0.5182	0.5806

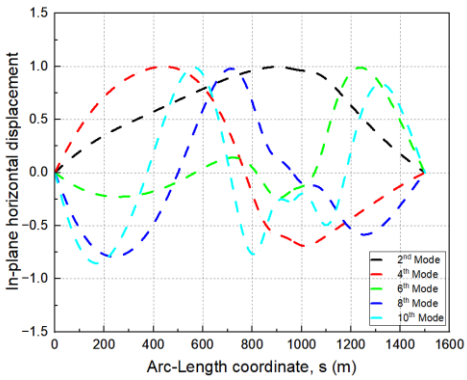

Fig. 10 Horizontal displacement for in-plane free vibration (x-direction)

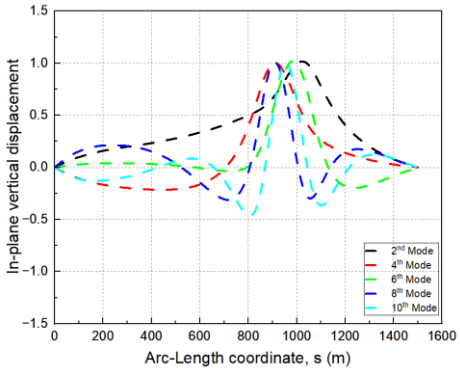

Fig. 11 Vertical displacement for in-plane free vibration (z-direction)

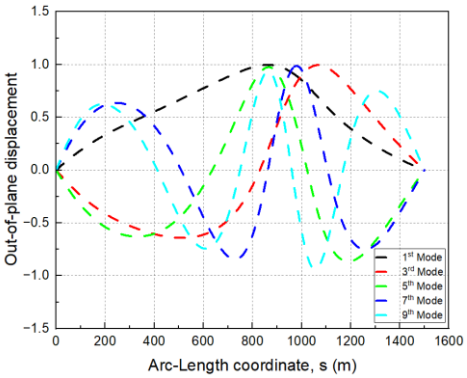

Fig. 12 Displacement for out-of-plane free vibration (y-direction)

The odd-numbered modes represent out-of-plane vibrations (y-direction), while the even-numbered modes represent in-plane vibrations (x-z plane). The separation of the riser's vibration modes can be identified by analyzing the dynamic displacement values, as illustrated in **Fig. 10-12**

7.2 Effects of Buoyancy Section Length

This subsection presents the effect of buoyancy section length on the static equilibrium and free vibration behaviour of the steep wave riser for the different lengths, including 300 m, 400 m, 500 m, 600 m, and 700 m. The of the parameters of SWR used for the analysis is given in **Table 3** (case 2)**.**

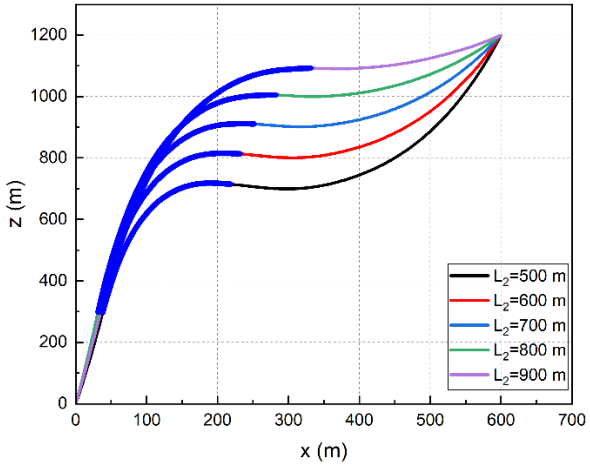

Fig. 13 Effect of buoyancy section on the configuration

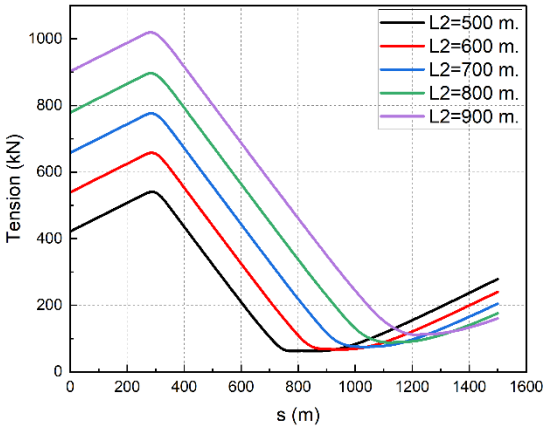

Fig. 14 Effect of buoyancy section length on the distribution of internal tension

The results demonstrate a correlation with the increase in the length of the buoyancy section. Specifically, the curvature of the wave riser section rises as the buoyancy section increases, as shown in **Fig. 13**.

The internal tension of the riser in the section without buoys also increases with the buoyancy section length increases, as shown in **Fig. 14**. Additionally, the natural frequency for the first ten vibration modes of the SWR is presented in **Table 5.**

Table 5 Effect of buoyancy section length on the natural frequency of SWR

Length of buoyancy section (m)	Natural frequencies, ω [rad/s]									
	Out-of-plane mode					In-plane mode				
	1st Mode	3rd Mode	5th Mode	7th Mode	9th Mode	2nd Mode	4th Mode	6th Mode	8th Mode	10th Mode
500	0.0991	0.1623	0.2373	0.3209	0.3991	0.1029	0.2127	0.2409	0.3530	0.4383
600	0.1022	0.1659	0.2344	0.3315	0.4100	0.1057	0.2309	0.2460	0.3805	0.4320
700	0.1088	0.1784	0.2710	0.3570	0.4472	0.1160	0.2212	0.2934	0.3986	0.4913
800	0.1126	0.1892	0.2877	0.3771	0.4750	0.1269	0.2176	0.3395	0.4021	0.5463
900	0.1171	0.2047	0.3078	0.4069	0.5096	0.1482	0.2160	0.3722	0.4467	0.5691

8. Conclusions

This study presents the influence of the buoyancy module characteristics on the free vibration response of the steep wave riser (SWR) in a Cartesian coordinate system, using a position vector that is a function of the riser's arc length coordinate.

The mathematical model is derived from the relationship between force equilibrium, moments, and strain along the tangent under the stretching rule of the riser with minimal deformation, known as the elastic rod model. The analysis of the SWR in deep subsea conditions with buoyancy modules is conducted in three dimensions. The analysis considers various forces acting on the riser, including the effective weight of the riser, the forces from sea currents, external seawater pressure, the internal flow velocity inside the pipe, and buoyancy forces from both the riser structure and buoyancy modules. A comprehensive mathematical model is developed to address related issues, which leads to the formulation of finite element equations using the Galerkin method. Since the system of equations is nonlinear, the Newton-Raphson iterative process is used to find numerical solutions. Natural frequencies are then analyzed using an eigenvalue problem, analyzed through MATLAB software to solve the equations.

In the final step, the results obtained are analyzed to determine the physical characteristics of the buoyancy modules that influence the static equilibrium state and the natural frequency of the riser. The calculated results, when compared with previous studies, the presented results are acceptable agreement. The related results are consistent with the increase in size and length of the buoyancy modules. The shape of the riser in the curved section (Wave riser) rises higher as the size and length of the buoyancy modules increase. Additionally, the internal tension in the riser in the section without buoyancy modules increases significantly as the diameter and length of the buoyancy section modules increase. The natural frequency for the first four modes are in the range from 0.1 – 0.3 rad/s Therefore, The riser should be designed with a natural frequency that avoids proximity to the frequency of external excitation forces, in order to reduce the likelihood of resonance.

Acknowledgement

The author would like to express sincere appreciation to the Department of Civil Engineering and the Faculty of Engineering at Kamphaeng Saen, Kasetsart University Kamphaeng Saen Campus, for the support through a research publication grant for an international academic journal and for their continued support of this research.

References

[1] Wu, M., & Huang, K. (2007). The Comparison of Various SCR Configurations For Bow Turret Moored FPSO In West Africa.

[2] Yang, H.-Z., & Li, H. (2011). Sensitivity analysis of fatigue life prediction for deepwater steel lazy wave catenary risers. Science China Technological Sciences, 54, 1881-1887. doi:10.1007/s11431-011-4424-y

[3] Kim, S., Kim, M. H., Shim, S., & im, S. (2014). Structural performance of deepwater lazy-wave steel catenary risers for FPSOs. Proceedings of the International Offshore and Polar Engineering Conference, 202-209.

[4] Bridge, C., Laver, K., Clukey, E., & Evans, T. (2004). Steel Catenary Riser Touchdown Point Vertical Interaction Models. doi:10.4043/16628-MS

[5] Clukey, E., & Zakeri, A. (2017). Recent Advances in Nonlinear Soil Models for Fatigue Evaluation of Steel Catenary Risers SCRs.

[6] Zhou, Z., O'Loughlin, C., & White, D. (2019). An effective stress analysis for predicting the evolution of SCR-seabed stiffness accounting for consolidation. Géotechnique, 70, 1-46. doi:10.1680/jgeot.18.p.313

[7] White, D. J., & Hodder, M. (2010). A simple model for the effect on soil strength of episodes of remolding and reconsolidation. Canadian Geotechnical Journal, 47(7), 821-826. doi:10.1139/T09-137

[8] Hodder, M. S., White, D. J., & Cassidy, M. J. (2013). An effective stress framework for the variation in penetration resistance due to episodes of remolding and reconsolidation. Géotechnique, 63(1), 30-43. doi:10.1680/geot.9.P.145

[9] Gao, Z., Wang, W., Zhou, Z., Yan, Y., & Pradhan, D. L. (2023). Dynamic response of a steel catenary riser at touch-down zone. Engineering Structures, 295, 116839. doi:https://doi.org/10.1016/j.engstruct.2023.116839

[10] Kim, H., & O'Reilly, O. (2019). Instability of catenary-type flexible risers conveying fluid in subsea environments. Ocean Engineering 173,98-115, doi.org/10.1016/j.oceaneng.2018.12.042

[11] Bai, Y., & Bai, Q. (2005). Subsea Pipelines and Risers. Subsea Pipelines and Risers. doi:10.1016/B978-0-08-044566-3.X5000-3

[12] Qiao, H., Ruan, W., Shang, Z., & Bai, Y. (2016). Non-Linear Static Analysis of 2D Steep Wave Riser Under Current Load. Offshore and Arctic Engineering. doi:10.1115/OMAE2016-54460